physica status solidi a
www.pss-a.com

Oxidation Behavior of Vanadium in Annealed AlCrVY(O)N Thin Films Characterized by X-ray Absorption Spectroscopy

Eric Schneider, Finn Ontrup, Gordon Scholz, Jaqueline Savelkouls, Nelson Filipe Lopes Dias, Christian Sternemann, Dirk Lützenkirchen-Hecht, Wolfgang Tillmann, and Michael Paulus*

Great efforts are being made to optimize tool coatings for use at elevated process temperatures. The reason for this is to enable machining with minimized lubrication quantities. During operation, temperatures between 300 and 1000 °C can occur depending on the material and tool design. Thus to enable the machining of high-strength materials, the tool coatings must be optimized with regard to their temperature resistance, which is also significantly affected by their oxidation properties. AlCrVY(O)N thin films are potential candidates for such coating applications as the addition of V to AlCrN favors the formation of so-called Magnéli phases at high temperatures, that is, V oxides with varying stoichiometry, to reduce friction. X-ray absorption spectroscopy is applied to characterize the oxidation behavior of V in the thin films prepared in a combined dcMS/HiPIMS process for as-deposited AlCrVY(O)N thin films and after thermal treatment in the ambient atmosphere. The V average oxidation state is determined by analyzing the pre-edge feature at the V K-edge. Systematic changes in preoxidation, a high oxidation resistance below 800 °C, and promoted V oxidation for higher preoxidized coatings above 800 °C are found.

1. Introduction

AlCrN thin films are well known for their high wear and oxidation resistance as well as high hardness.[1] This is achieved by integrating Al into the face-centered cubic (fcc) crystal lattice of CrN. The hardness of the metastable fcc-AlCrN phase increases up to an Al content of 67 to 80% of the total amount of metal atoms in the structure.[2] Exceeding this threshold, a metastable hexagonal close-packed (hcp) phase[3–5] is formed which is undesirable as it results in a loss of hardness and wear resistance, leading to reduced tribological properties.[6] Supplementing the solid solution of Al and Cr with a Y content of about 3.4 at.% can further enhance the hardness and thermal stability up to 1000 °C.[6–8] Doping of CrAlN thin films with Y leads to decelerated diffusion processes due to the segregation of Y at the grain boundaries, which significantly changes their oxidation behavior in a way that diffusion of elements from the layer to the surface and the diffusion of oxygen into the layer is hindered.[9] In order to reduce the friction on the surface of the thin film at high temperatures, V can be added to the solid solution which may form Magnéli phases of the type Me_nO_{2n-1} and Me_nO_{3n-1}.[10,11] The shear planes of these phases decrease the friction.[12,13] Tillmann et al. demonstrated that the optimal V content in AlCrVN solid solutions is 7.1 at.% in order to preserve the exceptional mechanical properties of the thin films.[14] Similar Cr-based coatings form AlCrON solid solutions due to small amounts of O. With higher O contents, additional solid solutions and amorphous phases are formed.[1,15,16] In addition, up to an O/(N + O) ratio of 0.69, the hardness and stability increase compared to AlCrN thin films.[17] For example, Gao et al.[18] have shown that the addition of oxygen into AlCrON coatings optimizes its adhesion strength with an impact on the service life of corresponding cutting tools. However, the general oxidation behavior of these complex materials is not yet fully understood.

In this study, the deposition of thin films is conducted using a hybrid physical vapor deposition (PVD) process that combines direct current magnetron sputtering (dcMS) with high-power impulse magnetron sputtering (HiPIMS). dcMS is known to produce thin films with low density and hardness, whereas HiPIMS results in the formation of denser and harder AlCrN thin films in

E. Schneider, G. Scholz, J. Savelkouls, C. Sternemann, M. Paulus
Fakultät Physik/DELTA
TU Dortmund University
44221 Dortmund, Germany
E-mail: eric.schneider@tu-dortmund.de

F. Ontrup, N. F. Lopes Dias, W. Tillmann
Institute of Materials Engineering
TU Dortmund University
44221 Dortmund, Germany

D. Lützenkirchen-Hecht
Fakultät für Mathematik und Naturwissenschaften
Fachgruppe Physik
University of Wuppertal
42119 Wuppertal, Germany

The ORCID identification number(s) for the author(s) of this article can be found under https://doi.org/10.1002/pssa.202400682.

DOI: 10.1002/pssa.202400682

comparison.[19] However, the deposition rates with the HiPIMS process are significantly lower than with dcMS. Depending on the peak current density, HiPIMS achieves only 25–30% of the deposition rate of dcMS.[20,21] Thus, the combination of both deposition techniques in a hybrid process is favorable to optimize the film properties. For example, one cathode can be operated with dcMS, while another is operated with HiPIMS[19,20,22] which has been demonstrated to be an effective method for depositing thin films with relatively high deposition rates as well as improved mechanical and tribological properties.[23–28]

In this study, the formation of V oxides during the combined dcMS/HiPIMS thin films process is triggered by injecting O_2 into the reactive sputtering process alongside N_2. The O_2 gas flow rate supplement during deposition was varied between 0 and 20 sccm to obtain different O contents within the AlCrVOYN thin films. The more or less preoxidized thin films were then gradually annealed up to a maximum temperature of 1000 °C in ambient atmosphere in order to characterize the oxidation behavior after the thermal exposure. For the analysis of the oxidation properties, X-ray near-edge absorption spectroscopy (XANES) at the V K-edge is applied which provides information on the average oxidation state of V both for only small amounts of V in the coating and also when noncrystalline V phases are present that cannot be detected by X-ray diffraction.

2. Experimental Section

2.1. Synthesis

The AlCrVY(O)N thin films have been deposited on rectangular WC-Co substrates with a size of $(14 \times 14 \times 4)$ mm^3, which were cleaned with ethanol in an ultrasonic bath for at least 10 min. The substrate was coated using an industrial magnetron sputtering system (type CC800/9, CemeCon AG, Germany). Al52Cr30V16.5Y1.5 targets (Plansee Composite Materials GmbH, Germany) with the dimensions (500×88) mm^2 were used for the deposition process. The dcMS/HiPIMS hybrid process was applied for deposition, in which two magnetron cathodes operate in dcMS mode and two in HiPIMS mode, respectively. The gas flow rates of O_2 and N_2 were measured and controlled individually before the gases were fed together into the process chamber. During the deposition of the AlCrVY(O)N thin films, the O_2 flow rate was varied between 0 and 20 sccm in steps of 5 sccm. The N_2 flow rate during coating was between 130 sccm. Argon was used as an ionization gas to keep the deposition pressure at 400 mPa during the deposition.

The average composition of the thin films determined by wavelength dispersive X-ray spectroscopy was determined to be 22 at.% Al, 15 at.% Cr, 7 at.% V, and 0.65 at.% Y. Starting with 0 sccm O_2, the N content was about 54 at.% while the O content was 1 at.%. With increasing O_2 flow rate up to 20 sccm, the O content in the thin film increases to about 21 at.% while the *N* content drops to 34 at.%. The layer thickness of the deposited thin films was between 2.4 and 2.7 µm. An example of the layer thickness at an O_2 flow of 10 sccm is shown in **Figure 1**.

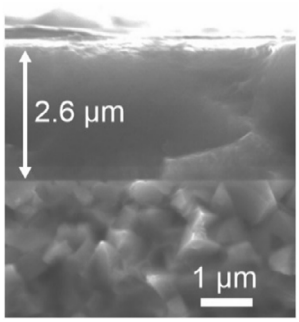

Figure 1. SEM image of the morphology of exemplarily chosen AlCrVYON thin film deposited from AlCrVY targets with a film thickness of 2.6 µm.

2.2. X-ray Absorption Measurements

In order to probe the oxidation behavior of the thin films at temperatures that appear during machining, the AlCrVY(O)N thin films were heated up to 1000 °C in 100 °C steps between 400 and 800 °C, and in 25 °C steps between 800 and 1000 °C using an SR 100-750/11 tube furnace (Carbolite Gero GmbH & Co. KG, Germany). The maximum annealing temperature was not reached for some thin films that chipped off the substrate. The samples were exposed for an entire heating period of 10 min and the temperature was controlled by temperature sensors close to the central part of the tube furnace with a temperature stability of ±3 °C.

The as-deposited and annealed thin films were investigated at the beamline BL10 of the synchrotron light source DELTA (Dortmund, Germany).[29] XANES spectra were measured via fluorescence detection by scanning the incident X-ray energy using a Si(111) channel-cut monochromator. The incident X-ray intensity was monitored by an ionization chamber filled with a mixture of He and N_2 (each with ≈50%) and a length of 15 cm, resulting in a transmission of about 90% at the energy of the V K-edge (5465 eV). The fluorescence radiation emitted from the samples was detected with a large-area passivated implanted planar silicon detector (Canberra, USA) having a diameter of 55 mm located above the sample. The incoming X-rays hit the sample at a grazing angle of 2°. The incident energy was varied in the vicinity of the V K absorption edge from 5345 to 5685 eV using a beam size of (0.2×8.0) mm^2 (v × h). Calibration of the energy scale was achieved by measurements of a *V* metal foil in transmission and defining the edge position as the first maximum of the derivative spectrum at $E = 5465$ eV.

The XANES measurements were conducted for the non-heated, as-deposited thin films and directly after each heating period, when cooled to room temperature in air. XANES spectra of different V oxide powders with different oxidation states (purity of 99% and more) served as references. We used powders of the oxides V_2O_3 (Thermo Fisher Scientific Inc., USA and Alfa Aesar, USA), V_2O_4 (MaTeck, Germany and Alfa Aesar, USA), and V_2O_5 (Thermo Fisher Scientific Inc., USA and Alfa Aesar, USA). The single XANES spectra were analyzed using the Demeter program package.[30]

2.3. Data Analysis

The V XANES spectra were extracted from the raw data by correcting for contribution from background and absorption of other atomic species contained in the sample. This was achieved using a linear fit between 70 and 20 eV below the edge-onset and removing the postedge background fitted between 75 and 218 eV above the edge along with a normalization of the edge jump to 1. In order to extract the pre-edge feature, an arctan function was fitted to model the main edge contribution and subtracted (see **Figure 2**ii). The extracted pre-edge feature was evaluated regarding its centroid energy position and its area in order to characterize the samples oxidation state according to the scheme discussed in e.g.[31–34]

3. Results and Discussion

The reference spectra are shown in Figure 2iii and demonstrate the characteristic changes appearing due to oxidation of V, that is, particularly the increase in prepeak intensity and shift of the main-edge onset to higher energies as well as changes in the postedge shape. Similar changes can be observed in the as-deposited and annealed AlCrVY(O)N thin films as shown in **Figure 3**i,ii, respectively. The pre-edge of the as-deposited thin films is more prominent with increasing O_2 flow rates applied during synthesis while the main-edge position shifts to higher energies suggesting that the AlCrVYON thin films are preoxidized for the O_2 flow rate above 10 sccm with stronger variation in the local environment of V at 20 sccm as indicated by the

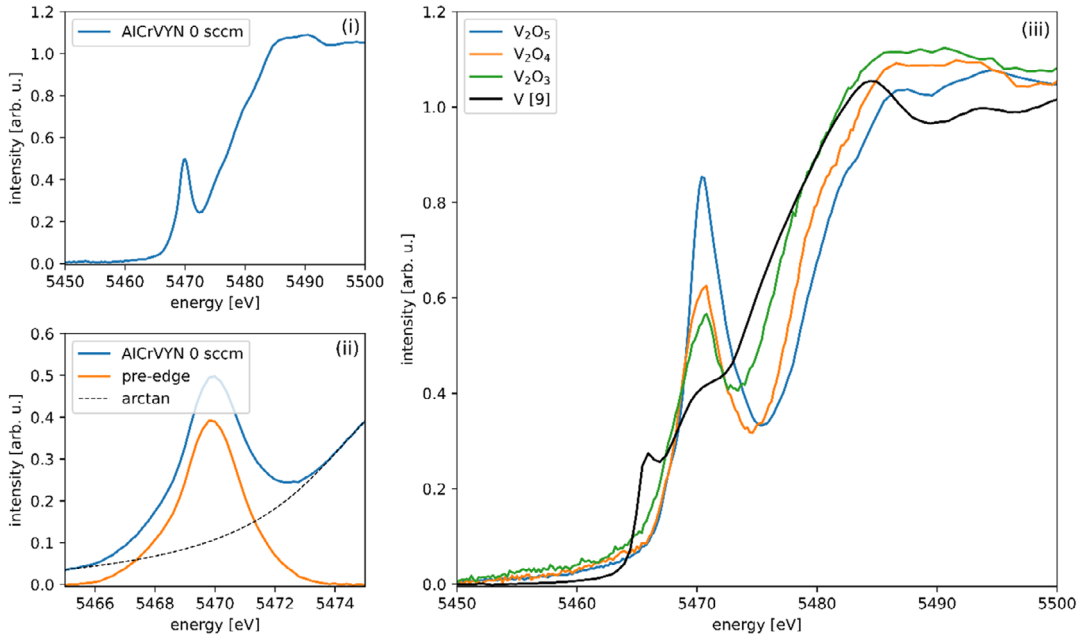

Figure 2. i) Typical XANES spectrum (normalized and background corrected) of an annealed AlCrVYN sample (top, left). ii) Extraction of the pre-edge feature using an arctan function to model the main-edge contribution (bottom, left). iii) Reference spectra of the different oxides and V metal, latter taken from.[10]

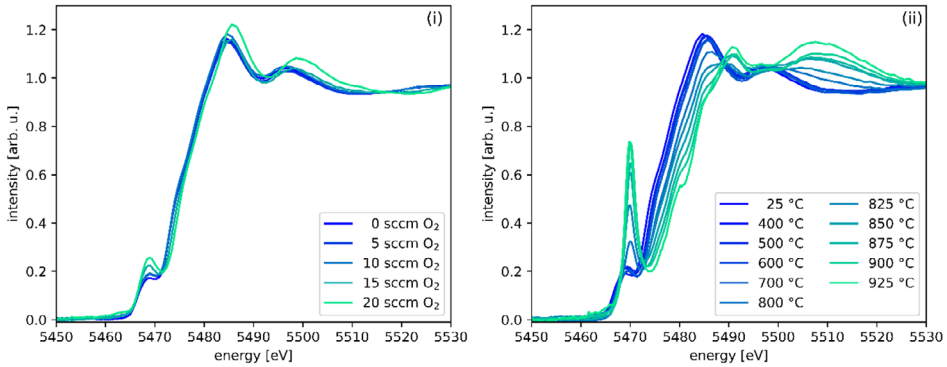

Figure 3. i) XANES spectra of the as-deposited AlCrVYON thin films produced at O_2 flow rates from 0 to 20 sccm (left). ii) XANES spectra of AlCrVYON thin film annealed in ambient atmosphere for the sample preoxidized at O_2 flow of 10 sccm for 10 min and the indicated temperatures (right).

changes in the postedge region. The typical variation of the V K-edge with temperature dependency is presented for the AlCrVYON thin film deposited with an O_2 flow rate of 10 sccm as an example in Figure 3ii. All other AlCrVYON thin films (not shown here) behave similar. We observe that the pre-edge intensity increases strongly at 700 °C accompanied by a significant main-edge shift to higher energies and corresponding changes in the postedge region. These changes are clear signs of the formation of new V phases with higher degrees of oxidation: Although the spectra of the oxide references exhibit similar behavior with increasing oxidation state, the overall shape of the spectra of the thin films is different due to differences in the local environment of V within AlCrVY(O)N. The vanadium occupies Cr atom positions in the solid solution having fcc structure. Thus, the V atoms with oxidation state III are surrounded by 6 N atoms. The structure of the vanadium K absorption edge in oxidation state III strongly depends on its local and chemical environment.[35] This leads to a change in the edge shape and particularly in the pre-edge depending on whether vanadium is considered being in a nitrogen environment or in an oxygen environment, for example, V_2O_3, which is less significant with higher oxidation states. Initially, V is assumed to be in oxidation state IIIN in a N environment corresponding to the sample prepared at 0 sccm and measured at room temperature. Changes in the pre-edge and main edge with respect to this reference spectrum are attributed to the formation of vanadium oxides (initially also in oxidation state III). Since the oxidation state of V in the solid solution and V_2O_3 is V[III], in V_2O_4 is V[VI] while it changes to V[V] in V_2O_5,[33] the pre-edge analysis provides a reasonable estimate on the average oxidation state when N is exchanged by O.

In order to characterize the average oxidation state of all thin films, the dependency of the integrated pre-edge feature's area and energy position is presented in **Figure 4** in comparison to the results obtained for the reference samples and new analysis of data published in ref. [14] using the current pre-edge extraction scheme. The average oxidation states III, IV, and V were defined using the V_2O_3, V_2O_4, and V_2O_5 by the average of present data and that analyzed taken from ref. [10], both measured in similar scattering geometry resulting in similar degree of self-absorption and are comparable to the results of Chaurand et al.[31] The gray-shaded areas indicate the range of uncertainty comparing different measurements performed in this work and analyzed data from ref. [10]. An overview of the corresponding values for the as-deposited and up to 925 °C annealed thin films can be found in **Table 1**. The highest average V oxidation state during annealing of the thin films is slightly above IV and is achieved by AlCrVYON produced at an O_2 flow rate of 15 sccm while the thin film produced at 5 sccm without proxidations reached a value of just above III. The oxidation behavior is characterized in more detail by inspecting the temperature dependency of the integrated area of the pre-edge as shown in Figure 4ii. Below 800 °C, we observe no change in peak area with rising temperature. However, AlCrVYON thin films produced with a higher O_2 flow rate show a larger area of the prepeak feature which is

Table 1. Area and centroid energy position of the prepeak feature determined for as-deposited and annealed AlCrVY(O)N thin films.

Coating	O_2 content [sccm]	Temperature [°C]	Pre-edge area	Pre-edge centroid position [eV]
AlCrVYN	0	25	0.41 ± 0.05	5468.2 ± 0.1
AlCrVYN	0	925	1.63 ± 0.06	5470.5 ± 0.1
AlCrVYON	5	25	0.42 ± 0.05	5468.4 ± 0.1
AlCrVYON	5	925	1.6 ± 0.2	5470.3 ± 0.1
AlCrVYON	10	25	0.42 ± 0.05	5468.4 ± 0.1
AlCrVYON	10	925	2.0 ± 0.1	5470.1 ± 0.1
AlCrVYON	15	25	0.59 ± 0.1	5468.6 ± 0.1
AlCrVYON	15	925	2.29 ± 0.05	5470.0 ± 0.1
AlCrVYON	20	25	0.71 ± 0.05	5468.6 ± 0.1
AlCrVYON	20	900	1.83 ± 0.09	5470.4 ± 0.1

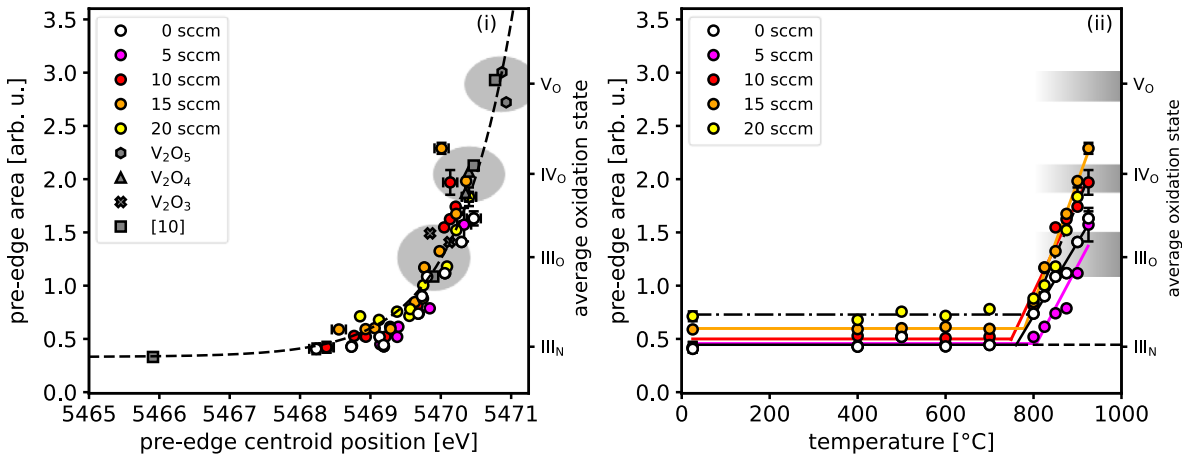

Figure 4. i) Average oxidation state of AlCrVYON thin films characterized by the area and centroid position of the prepeak feature constrained by the V oxides (oxidation states III_O, IV_O, and V_O), V metal, and AlCrVYON 0 sccm reference (oxidation state III_N) samples (left). Squares indicate analyzed data taken from ref. [10]. Gray-shaded areas indicate the fields of uncertainty for referencing the oxidation state. Error bars are shown for selected data. ii) Intensity change of the prepeak feature with temperature (right). Lines are fits of a constant and a linear increase up to 700 °C and above 800 °C, respectively, as guide to the eye (right). Error bars are shown for selected data.

particularly pronounced for the thin films sputtered at an oxygen flow rate of 10 and 15 sccm, while the thin films produced at 0 and 5 sccm do not differ from each other. This can be related to different stages of preoxidation during the thin film synthesis which is maintained in a large temperature range. From around 800 °C, we see an almost linear increase of the intensity with temperature and confirm that the thin films with higher degree of preoxidation reach a higher average oxidation state at the same annealing conditions.

All AlCrVY(O)N thin films, preoxidized or not, exhibit high oxidation resistance up to temperatures of 700–800 °C. From around 800 °C, the V in thin films with higher degree of preoxidation oxidizes faster and thus reaches higher average oxidation state at the maximum annealing temperature. This aligns with the higher degree of O incorporated in the preoxidized thin films on cost of the nitrogen content. Consequently, we find clear indication that the appearance of larger amount of O in the AlCrVYON thin film after the dcMS/HiPIMS process promotes the V oxidation, that is, the formation of Magnéli phases.

4. Conclusion

In this work, we studied the average oxidation state of V in AlCrVY(O)N thin films synthesized with systematically varying the O_2 flow rates in the reactive atmosphere using a hybrid dcMS/HiPIMS deposition process and probed the oxidation properties of the as-deposited thin film during annealing up to 925 °C in ambient atmosphere using XANES. Within the sputtering process, the oxygen content in the AlCrVYON thin film can be well tuned. All as-deposited thin films show a high oxidation resistance of V below temperatures of 800 °C. For higher temperatures, the degree of preoxidation affects the oxidation characteristics of the thin films, that is, preoxidation promotes the formation of V oxides with higher valence. This makes the preoxidation in the dcMS/HiPIMS process a valuable tool for directed oxidation in order to optimize the tribological properties and represents a pathway in the production of friction-reducing thin films based on vanadium oxide.

Acknowledgements

The authors thank DELTA for providing synchrotron radiation and the DELTA machine group for technical support. This work was supported by the German Research Foundation via TO 169/21-1 and TI 343/190-1.

Open Access funding enabled and organized by Projekt DEAL.

Conflict of Interest

The authors declare no conflict of interest.

Data Availability Statement

The data that support the findings of this study are available from the corresponding author upon reasonable request.

Keywords

AlCrVYON, magnetron sputtering, thin films, vanadium oxides, X-ray absorption spectroscopy

Received: August 29, 2024
Revised: December 5, 2024
Published online: December 22, 2024

[1] J. Vetter, A. O. Eriksson, A. Reiter, V. Derflinger, W. Kalss, *Coatings* **2021**, *11*, 344.
[2] N. Bagcivan, K. Bobzin, S. Theiß, *Thin Solid Films* **2013**, *528*, 180.
[3] A. Sugishima, H. Kajioka, Y. Makino, *Surf. Coat. Technol.* **1997**, *97*, 590.
[4] R. Kaindl, R. Franz, J. Soldan, A. Reiter, P. Polcik, C. Mitterer, B. Sartory, R. Tessadri, M. O'Sullivan, *Thin Solid Films* **2006**, *515*, 2197.
[5] Y. Makino, K. Nogi, *Surf. Coat. Technol.* **1998**, *98*, 1008.
[6] J. Tian, C. Hu, L. Chen, Y. Lou, N. Zhao, *Trans. Nonferrous Met. Soc. China* **2021**, *31*, 2740.
[7] F. Rovere, P. H. Mayrhofer, *J. Vac. Sci. Technol. A* **2007**, *25*, 1336.
[8] T. C. Rojas, S. Domínguez-Meister, M. Brizuela, J. C. Sánchez-López, *J. Alloys Compd.* **2019**, *773*, 1172.
[9] L. A. Donohue, I. J. Smith, W.-D. Münz, I. Petrov, J. E. Greene, *Surf. Coat. Technol.* **1997**, *94–95*, 226.
[10] W. Tillmann, D. Kokalj, D. Stangier, M. Paulus, C. Sternemann, M. Tolan, *Appl. Surf. Sci.* **2018**, *427*, 511.
[11] B. Stegemann, M. Klemm, S. Horn, M. Woydt, *Beilstein J. Nanotechnol.* **2011**, *2*, 59.
[12] N. Fateh, G. A. Fontalvo, G. Gassner, C. Mitterer, *Wear* **2007**, *262*, 1152.
[13] V. Perfilyev, A. Moshkovich, I. Lapsker, A. Laikhtman, L. Rapoport, *Wear* **2013**, *307*, 44.
[14] W. Tillmann, D. Kokalj, D. Stangier, M. Paulus, C. Sternemann, M. Tolan, *Surf. Coat. Technol.* **2017**, *328*, 172.
[15] H. Najafi, A. Karimi, E. Oveisi, M. Morstein, *Thin Solid Films* **2014**, *572*, 176.
[16] M. Stüber, U. Albers, H. Leiste, K. Seemann, C. Ziebert, S. Ulrich, *Surf. Coat. Technol.* **2008**, *203*, 661.
[17] Z. R. Liu, J. W. Du, L. Chen, *Surf. Coat. Technol.* **2022**, *432*, 128057.
[18] Y. Gao, F. Cai, W. Fang, Y. Chen, S. Zhang, Q. Wang, *J. Mater. Eng. Perform* **2019**, *28*, 828.
[19] K. Bobzin, T. Brögelmann, N. C. Kruppe, M. Engels, *Thin Solid Films* **2016**, *620*, 188.
[20] U. Helmersson, M. Lattemann, J. Bohlmark, A. P. Ehiasarian, J. T. Gudmundsson, *Thin Solid Films* **2006**, *513*, 24.
[21] J. Vetter, T. Shimizu, D. Kurapov, T. Sasaki, J. Mueller, D. Stangier, M. Esselbach, *J. Appl. Phys.* **2023**, *134*, 160701.
[22] J. Paulitsch, P. H. Mayrhofer, W.-D. Münz, M. Schenkel, *Thin Solid Films* **2008**, *517*, 1239.
[23] H. Zhou, J. Zheng, B. Gui, D. Geng, Q. Wang, *Vacuum* **2017**, *136*, 129.
[24] M. S. Kang, T. Wang, J. H. Shin, R. Nowak, K. H. Kim, *Trans. Nonferrous Met. Soc. China* **2012**, *22*, s729.
[25] B. Gui, H. Zhou, J. Zheng, X. Liu, X. Feng, Y. Zhang, L. Yang, *Ceram. Int.* **2021**, *47*, 8175.
[26] J. Paulitsch, M. Schenkel, T. Zufraß, P. H. Mayrhofer, W.-D. Münz, *Thin Solid Films* **2010**, *518*, 5558.
[27] W. Tillmann, F. Ontrup, E. Schneider, M. Paulus, C. Sternemann, N. F. Lopes Dias, *Hybrid Adv.* **2024**, *5*, 100120.
[28] N. F. Lopes Dias, A. L. Meijer, D. Biermann, W. Tillmann, *Surf. Coat. Technol.* **2024**, *487*, 130987.
[29] D. Lützenkirchen-Hecht, R. Wagner, S. Szillat, A. K. Hüsecken, K. Istomin, U. Pietsch, R. Frahm, *J. Synchrotron Radiat.* **2014**, *21*, 819.

[30] B. Ravel, M. Newville, *J. Synchrotron Radiat.* **2005**, *12*, 537.
[31] P. Chaurand, J. Rose, V. Briois, M. Salome, O. Proux, V. Nassif, L. Olivi, J. Susini, J.-L. Hazemann, J.-Y. Bottero, *J. Phys. Chem. B* **2007**, *111*, 5101.
[32] G. Giuli, E. Paris, J. Mungall, C. Romano, D. Dingwell, *Am. Miner.* **2004**, *89*, 1640.
[33] S. R. Sutton, J. Karner, J. Papike, J. S. Delaney, C. Shearer, M. Newville, P. Eng, M. Rivers, M. D. Dyar, *Geochim. Cosmochim. Acta* **2005**, *69*, 2333.
[34] M. Wilke, F. Farges, P. Petit, G. Brown, F. Martin, *Am. Miner.* **2001**, *5*, 714.
[35] E. J. O'Loughlin, M. I. Boyanov, K. M. Kemner, *Minerals* **2021**, *11*, 316.